

Nonlinear light absorption in colloidal CdSe/CdS nanoplatelets

V. N. Mantsevich,^{1,*} D. S. Smirnov,² A. M. Smirnov,³ A. D. Golinskaya,¹
M. V. Kozlova,¹ B. M. Saidjonov,¹ V. S. Dneprovskii,¹ and R. B. Vasiliev¹

¹*Lomonosov Moscow State University, 119991 Moscow, Russia*

²*Ioffe Institute, 194021, St. Petersburg, Russia*

³*Kotel'nikov Institute of RAS, 125009 Moscow, Russia*

We investigated the nonlinear optical properties of CdSe/CdS nanoplatelets in the vicinity of heavy hole and light hole exciton resonances. The two color pump-probe technique was applied. The first intense pulse created non-equilibrium exciton population, which was detected as a decrease of probe light absorption. We observed intense scattering of excitons between heavy- and light-hole excitonic states. We also studied experimentally saturation of absorption in nanoplatelets. Theoretical description of these phenomena allowed us to determine parameters of exciton dynamics in nanoplatelets.

I. INTRODUCTION

Semiconductor nanocrystals attract a great deal of attention due to their physical and chemical properties promising for optoelectronic applications [1]. Nanocrystals can be conveniently grown by colloidal synthesis, which allows to precisely control their shape [2], size [3] and crystal structure [4]. Recently, this approach was applied to synthesize finite size semiconductor quantum wells, which are called nanoplatelets (NPLs) [5]. NPLs demonstrate strong quantum confinement of charge carriers, because their thickness along [001] axis is of the order of several monolayers [5], which can be used to tune the optical absorption and photoluminescence spectra [6–10]. NPLs exhibit a large exciton binding energy [11, 12] and demonstrate a number of other remarkable properties such as narrow emission lines even at room temperature, tunable emission wavelength, short radiative lifetimes, giant oscillator strength, high quantum yield and vanishing inhomogeneous broadening [13–17]. This makes NPLs very attractive for application in future optoelectronic devices as bright and flexible light emitters [8, 18], as colloidal lasers [11, 19] or for biomedical labeling [20].

Despite a set of potential applications of colloidal NPLs, experimental investigation of their fundamental properties was mainly focused on the time ranges of the excited states dynamics, such as decay pathways of the single-exciton state [12, 21], recombination dynamics of band edge excitons [16], non-radiative Auger recombination [11, 23] or photoluminescence decay dynamics [24, 25]. In the same time various possible applications of NPLs in optical devices calls for detailed investigation of their nonlinear optical properties at high (room) temperature [26–28]. This however have hardly been done up to date.

In this work, we study nonlinear transmission of CdSe/CdS NPLs with different shell thicknesses. We observe bleaching of excitonic transitions and saturation of exciton population in NPL using two color pump probe

technique. This paper is organized as usual: In Sec. II we describe the procedure of colloidal synthesis of NPLs and their structure properties. Then in Sec. III we present experimental setup and experimental results, which are theoretically analyzed in Sec. IV. Comparison of theoretical predictions and experimental results allowed us to estimate parameters of exciton dynamics including average exciton lifetime and radiative recombination rate. Our main experimental and theoretical findings are summarized in concluding Sec. V.

II. SYNTHESIS AND STRUCTURAL CHARACTERIZATION OF NANOPLATELETS.

CdSe NPLs having five monolayer (5ML) thickness were synthesized by the modified method adapted from Ref. 5. In a typical synthesizes 0.5 mmol cadmium acetate, 0.2 mmol of oleic acid (OA) and 10 mL of octadecene (ODE) were introduced into a reaction flask. The mixture was degassed under magnetic stirring and argon flow at 180°C during 30 minutes. Then, the temperature was raised to 210°C and 0.2 mmol trioctylphosphine (TOP) Se solution was quickly injected into the mixture. The growth time of NPLs was 40 minutes at 210°C. The mixture was then cooled down to room temperature and 1 mL of OA was injected. As-synthesized CdSe NPLs were precipitated by adding an equal volume of acetone and centrifugation at 7000 rpm for 5 min and washed two times with acetone. Finally, NPLs precipitates were re-dispersed in 6 mL of hexane.

The synthesis of CdSe/CdS heterostructures was carried out by the method of low-temperature layer-by-layer deposition of shell material according to Ref. 29. Briefly, 1 mL of a solution CdSe NPLs in hexane and 1 mL a freshly prepared 0.1 M solution of Na₂S in N-methylformamide (NMF) were mixed and shaken for 1 hour. At the same time, a transfer of nanoparticles from the nonpolar hexane phase to the polar NMF phase was observed, which means the exchange of oleic ligands at the surface of NPLs by a monolayer of S²⁻. The polar phase was rinsed several times with hexane and then

* vmantsev@gmail.com

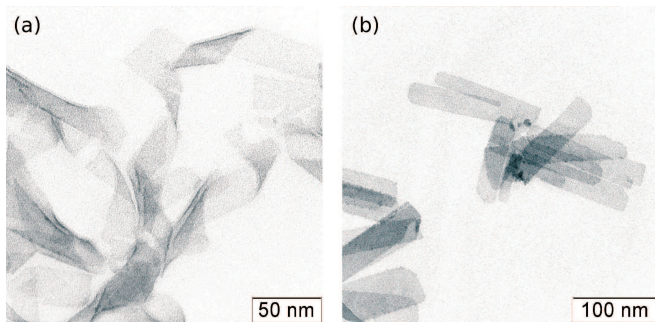


FIG. 1. Low-resolution transmission electron microscopy (TEM) overview images of as-synthesized CdSe NPLs (a) and CdSe/CdS NPLs with 2 ML of CdS on each of basal planes (b).

the NPLs were precipitated by adding a mixture of acetonitrile and toluene (1 : 1 by volume) followed by centrifugation at 7000 rpm and redispersed in NMF. The precipitation-redispersion cycles were repeated two times to purify the residues from unreacted sulfur-ions. Then 1 mL of a solution 0.3 M of $\text{Cd}(\text{OAc})_2 \cdot 2\text{H}_2\text{O}$ in NMF was added to the precipitate and left for 40 minutes to grow a CdS monolayer. The procedure described above corresponds to the synthesis of a single CdS monolayer. To obtain 5CdSe/2CdS heterostructures, this process was repeated two times. The synthesized NPLs were investigated experimentally in a liquid solution of methylformamide.

Low-resolution transmission electron microscopy (TEM) image of as-grown CdSe NPLs [Fig. 1(a)] demonstrates two-dimensional morphology. Rectangle platelets with lateral sizes about 30×100 nm rolled up into nanoscrolls. Fig. 1(b) presents typical image of CdSe NPLs after covering with 2 ML of CdS. We found that initially rolled NPLs unfolded into flat nanostructures. As a result well-defined rectangle CdSe/CdS platelets with the same lateral sizes as CdSe NPLs were formed. The synthesized NPLs had zinc-blend crystal structure [30].

III. EXPERIMENT

We study nonlinear optical properties of NPLs at room temperature using pump-probe technique. Pumping was realized by the mode-locked $\text{Nd}^{3+}:\text{YAlO}_3$ laser second harmonic ($\lambda = 540$ nm, pulse duration about 10 ns). As a probe we used a broadband photoluminescence radiation of the Coumarin-7 and Kiton Red dyes excited by the third harmonic ($\lambda = 360$ nm) of the pumping laser [31]. The probe pulse duration was 11 ns, and we adjusted it to overlap with the pump pulse, as shown in Fig. 2(a). Because of relatively long pulse duration we probe steady state of the system. The broad spectrum of the pump light is shown in Fig. 2(b), it covers wavelengths from 480 to 600 nm by Coumarin-7 photoluminescence and from 590 to 660 nm by Kiton Red photoluminescence.

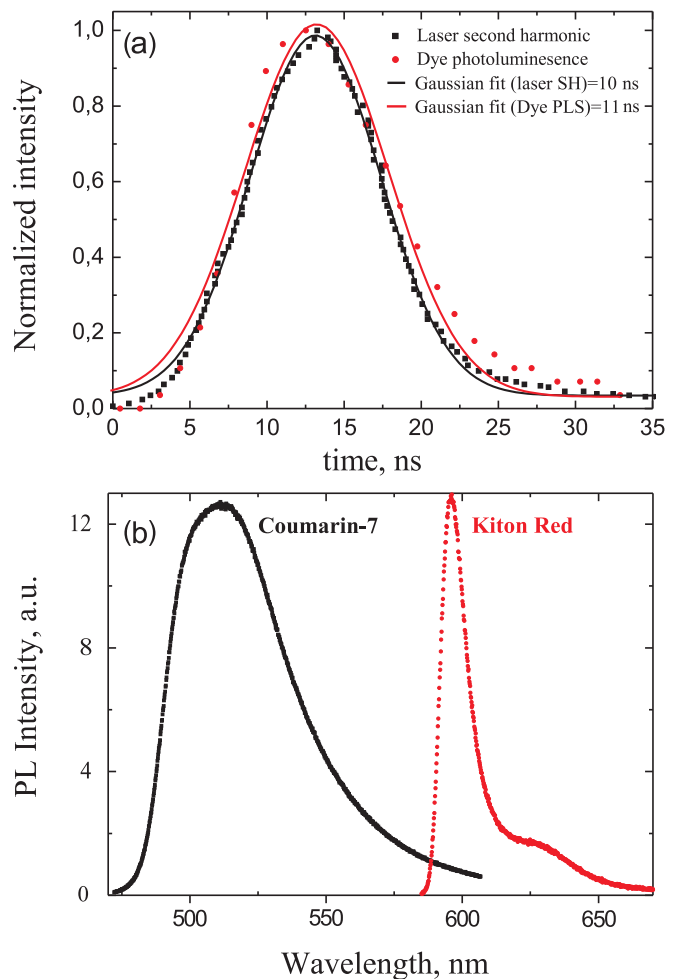


FIG. 2. (a) The temporal profiles of the pump (red dots) and the probe (black dots) pulses. The curves show the corresponding Gaussian fits. (b) Spectra of the probe pulse, being the photoluminescence spectra of Coumarin-7 or Kiton Red dyes.

The transmission and absorption of the probe light was measured with spectral resolution using SpectraPro 2300i spectrometer with PIXIS 256 CCD-camera. The absorption spectra of 5CdSe/CdS and 5CdSe/2CdS NPLs (5 core CdSe monolayers with 1 or 2 CdS shell monolayers, respectively) in 1 mm cell with methylformamide in the absence of pumping are shown in Fig. 3. The two pronounced peaks correspond to the heavy- and light-hole excitons [21]. The energies of these transitions are determined by the size quantization in direction perpendicular to NPLs. One can see, that the two peaks shift in 5CdSe/2CdS NPLs with respect to 5CdSe/CdS NPLs because of the deeper penetration of the exciton wavefunction in CdS shell.

The wavelength of the pump laser is shown by the green arrow in Fig. 3. One can see that it corresponds to heavy hole (hh-e) and light-hole (lh-e) transitions in 5CdSe/CdS and 5CdSe/2CdS NPLs, respectively. As a result the pump light resonantly excites the correspond-

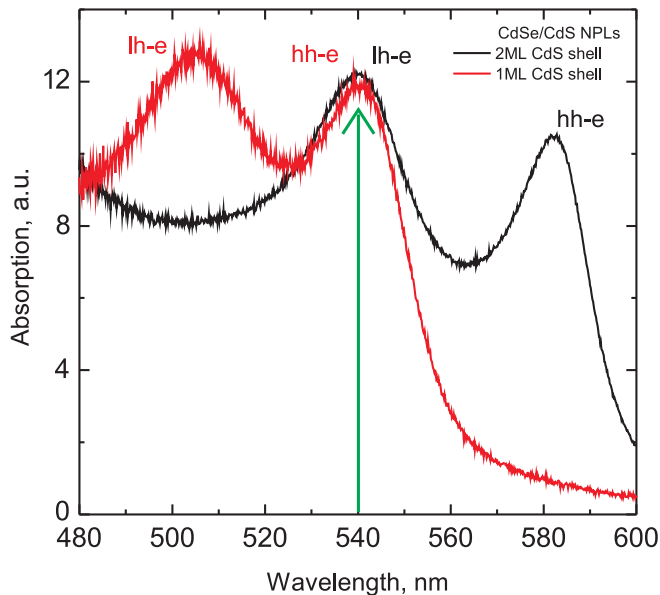


FIG. 3. Absorption spectra of colloidal solution of 5CdSe/CdS and 5CdSe/2CdS NPLs. Green arrow shows the pump laser wavelength.

ing excitonic states in the two studied samples.

The transmission spectra of the probe light for different pump powers are shown in Fig. 4. Here one can see two dips corresponding again to hh-e and lh-e transitions. Increase of the pump power leads to the eventual disappearance of the dips. Fig. 5 demonstrates transmission as a function of pump intensity for both samples at the hh-e and lh-e exciton transitions wavelength.

We introduce the differential transmission at a given wavelength λ as

$$DT(\lambda) = \frac{T_I(\lambda) - T_0(\lambda)}{T_0(\lambda)}, \quad (1)$$

where $T_I(\lambda)$ is the transmission of the solution of colloidal NPLs under pumping with intensity I at the wavelength λ . The differential transmission spectra are shown in Fig. 6. They directly reflect nonlinear optical properties of colloidal NPLs. In particular we note that under strong excitation of heavy hole excitons [panel (a)] the differential transmission relevant to the same transition saturates. This suggests to develop a quantitative description of the observed phenomena.

IV. THEORY AND DISCUSSION

The optical transitions related to hh-e and lh-e are well resolved even at room temperature (see Fig. 3). This evidences large exciton binding energy and strong oscillator strength due to quantum confinement in perpendicular to NPL direction. In the previous section we presented results of nonlinear absorption of light under resonant excitation of heavy-hole and light-hole excitons. Interest-

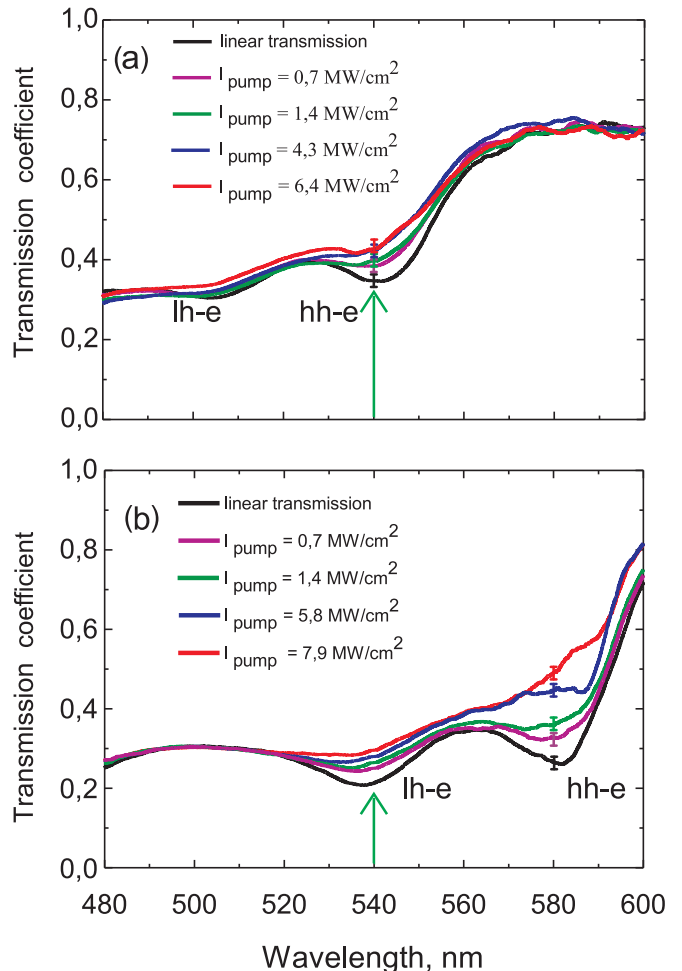


FIG. 4. Transmission spectra of (a) 5CdSe/CdS and (b) 5CdSe/2CdS NPLs. The green arrow corresponds to the pump wavelength. The vertical bars demonstrate the characteristic statistical error.

ingly in both cases the differential transmission is nonzero at both resonances. This means that after resonant excitation not only light hole excitons can scatter to the heavy hole excitonic states with lower energies, but also the inverse process takes place. As a result the system under study can be qualitatively described by the scheme shown in Fig. 7. In our experiment we did not observe any traces of trapping of charges at defect sites [21, 27], so we do not take this effect into account in this model.

The differential transmission can be related to three mechanisms [35] (i) phase space filling, (ii) screening of Coulomb interaction or (iii) broadening of the excitonic line. All three effects appear because of exciton-exciton interaction. For the following analysis we assume, that (i) differential transmission is proportional to the number of excitons in the corresponding state, and (ii) the times of exciton scattering between heavy-hole and light-hole states [τ_{down} and τ_{up} , see Fig. 7] are the shortest timescales in the system. These assumptions are made to obtain the simplest theoretical description of the sys-

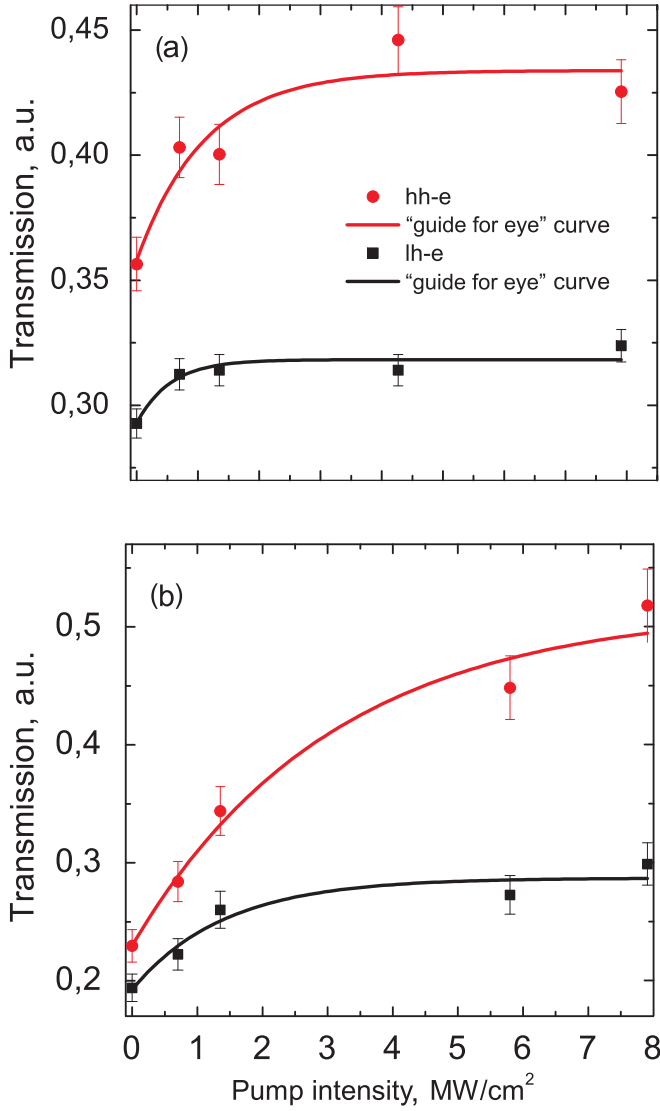


FIG. 5. Transmission as a function of pump intensity for the (a) 5CdSe/CdS nanoplatelets and (b) 5CdSe/2CdS nanoplatelets. Experimental dots correspond to the transmission spectra amplitudes maxima obtained under resonant excitation (see Fig.3).

tem, which can yield estimations for the parameters of exciton dynamics. Moreover we note, that exciton fine structure [36] can be neglected at room temperature [21].

The ratio of areas of differential transmission peaks corresponding to heavy- and light-hole excitons is

$$\frac{A_{hh}}{A_{lh}} = \frac{N_{hh}}{N_{lh}}, \quad (2)$$

where N_{hh} and N_{lh} are the concentrations of heavy- and light-hole excitons in NPLs, respectively. The balance of transitions between excitonic states reads

$$\frac{N_{hh}}{\tau_{up}} = \frac{N_{lh}}{\tau_{down}}. \quad (3)$$

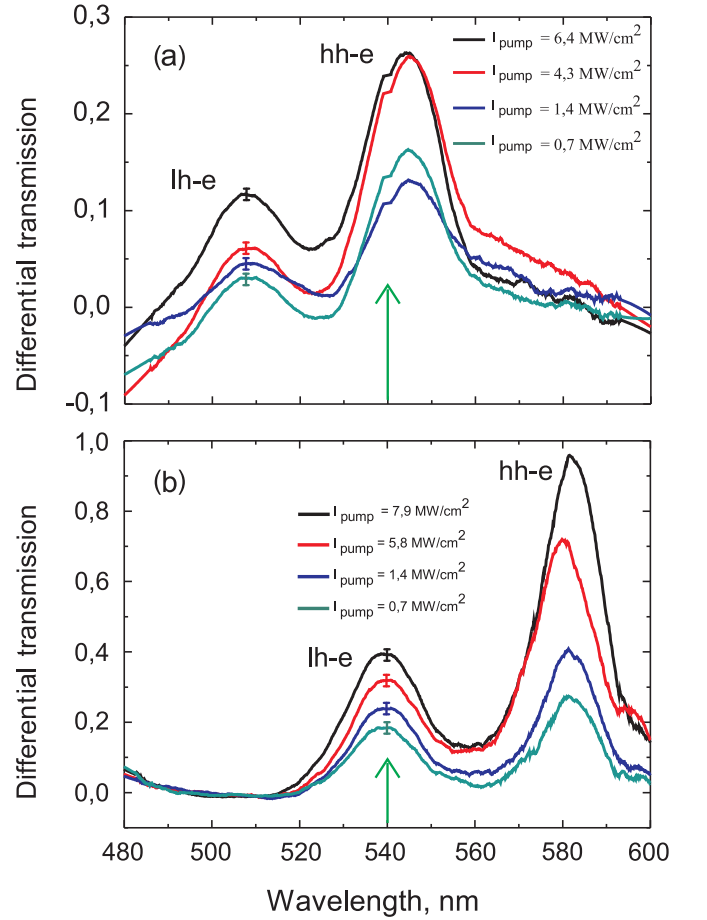


FIG. 6. The differential transmission spectra calculated after Eq. (1) for the different pump powers. Panel (a) corresponds to 5CdSe/CdS NPLs and panel (b) to 5CdSe/2CdS NPLs. Laser excitation parameters correspond to the one, shown in Fig. 4. The vertical bars demonstrate the characteristic statistical error.

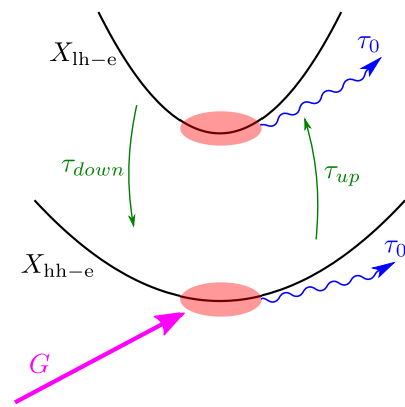


FIG. 7. Energy diagram of heavy hole (X_{hh-e}) and light hole (X_{lh-e}) excitons for resonant excitation of heavy-hole exciton. The red ovals show the part of exciton spectrum, where radiative decay takes place.

Accordingly one can find the ratio between the times of

exciton scattering to upper and lower energies as

$$\frac{\tau_{up}}{\tau_{down}} = \frac{A_{hh}}{A_{lh}}. \quad (4)$$

This ratio is about 1.5 for 5CdSe/CdS NPLs and about 2.5 for 5CdSe/2CdS NPLs.

We note that τ_{up}/τ_{down} is much smaller, than the Boltzmann exponent for the corresponding splitting between heavy-hole and light-hole excitonic states (≈ 160 meV). Therefore we conclude, that exciton scattering is induced by exciton-exciton interaction.

Under resonant excitation of heavy-hole excitons we observe saturation of differential transition at corresponding wavelengths, see Fig. 6(a). This effect is absent for resonant excitation of light-hole excitons, which is in agreement with the faster exciton scattering to lower than to higher energies, $\tau_{down} < \tau_{up}$. Let us study the saturation effect in more detail.

The saturation of differential transmission is related with the saturation of heavy-hole excitons concentration at [37]

$$N_s = \frac{7}{8\pi a_B^2}, \quad (5)$$

where a_B is the 3D Bohr radius, which is two times bigger, than the excitonic Bohr radius in narrow NPLs. The exciton generation rate G is given by

$$G = \frac{P_S}{\hbar\omega_0} \frac{2\Gamma_0}{\Gamma}, \quad (6)$$

where ω_0 is the pump carrier frequency and $2\Gamma_0/\Gamma$ is the absorbance of the nanoplatelet with Γ_0 and Γ being, respectively, radiative and nonradiative damping rates [38].

The radiative exciton decay can take place only in the so-called radiative cone — an area in the momentum space with small enough momenta [16, 39]. This area is schematically shown by red ovals in Fig. 7. The exciton radiative recombination time τ_0 is given by [40]

$$\frac{1}{\tau_0} = 2\Gamma_0 = \frac{4q^3}{3\varepsilon_b\hbar} |\mathcal{D}|^2, \quad (7)$$

where ε_b is the dielectric constant of the solution [41], $q = \sqrt{\varepsilon_b}\omega_0/c$ is the light wavevector with c being the speed of light in vacuum, and

$$|\mathcal{D}|^2 = \frac{4e^2 E_P A}{\pi\omega_0^2 m_0 a_B^2}. \quad (8)$$

Here e is the electron charge, E_P is the energy parameter measuring the Kane interband momentum matrix element, A is the area of NPL, m_0 is the free electron mass, and it is assumed that $Aq^2 \ll 1$.

Finally the average exciton lifetime τ can be estimated from the balance of exciton generation and recombination rates as

$$G = \frac{N_{hh} + N_{lh}}{\tau}. \quad (9)$$

Under saturation conditions one finds

$$\tau = \frac{N_s}{G} \left(1 + \frac{\tau_{down}}{\tau_{up}} \right), \quad (10)$$

where we have taken into account Eq. (3). For estimations we use the following parameters: $\hbar\omega_0 = 2.3$ eV, $\varepsilon_b = 2$, $A = 3000$ nm², $a_B = 5.6$ nm [42] and $E_P = 23$ eV [43]. We obtain $\hbar\Gamma_0 = 87$ μ eV, which corresponds to radiative lifetime of an exciton at rest (with zero in plane momentum) $\tau_0 = 3.8$ ps. The short radiative lifetime is related to relatively large area of NPLs, see Eq. (8). From Fig. 5 one can also estimate $P_S = 4$ MW/cm² and the exciton linewidth $\hbar\Gamma = 40$ meV, which from Eqs. (6) and (10) gives the average exciton lifetime $\tau \approx 24$ ps in agreement with Ref. [16]. We recall, that the significant difference between τ_0 and τ is related to the fact that the radiative decay of excitons is possible only inside the narrow radiative cone.

V. CONCLUSION

We studied experimentally nonlinear absorption and transmission of light in ensembles of CdSe/CdS NPLs. We used the two-color pump-probe technique with long pulse duration, which allowed us to study quasi steady state. Resonant excitation of heavy- and light-hole excitonic states revealed surprisingly small ratio of exciton scattering times to higher and lower energies. This is related to the nonlinear exciton scattering induced by exciton-exciton interaction.

We also observed saturation of differential transmission at heavy-hole exciton resonance. Theoretical analysis of this phenomenon allowed us to obtain average exciton lifetime and radiative recombination rate at room temperature. We believe, that investigation of nonlinear optical properties of colloidal NPLs performed in this paper will give a push to development of optoelectronic devices operating at room temperature on the basis of colloidal NPLs.

VI. ACKNOWLEDGEMENTS

We thank E. L. Ivchenko and A. A. Golovatenko for fruitful discussions and acknowledge the support by the RFBR grants 16 – 29 – 11694 and 18 – 02 – 00719. D.S.S. was partially supported by the Russian Foundation for Basic Research (Grant No. 17-02-0383), RF President Grant No. SP-643.2015.5, and the Basis Foundation.

-
- [1] M. Xu, T. Liang, M. Shi, H. Chen, *Chem. Rev.* **113**, 3766, (2013).
- [2] L. Manna, D. J. Milleron, A. Meisel, E. C. Scher, A. P. Alivisatos, *Nat. Mater.* **2**, 382, (2003).
- [3] C. B. Murray, D. J. Norris, M. G. Bawendi, *J. Am. Chem. Soc.* **115**, 8706, (1993).
- [4] X. Michalet, *Science* **307**, 538, (2005).
- [5] S. Ithurria, B. Dubertret, *J. Am. Chem. Soc.* **130**, 16504, (2008).
- [6] M. A. Hines, P. Guyot-Sionnest, *J. Phys. Chem.* **100**, 468, (1996).
- [7] D. V. Talapin, I. Mekis, S. Gotzinger, A. Kornowski, O. Benson, H. Weller, *J. Am. Chem. B* **108**, 18826, (2004).
- [8] Y. Chen, J. Vela, H. Htoon, J. L. Casson, D. J. Werder, D. A. Bussian, V. I. Klimov, J. A. Hollingsworth, *J. Am. Chem. Soc.* **130**, 5026, (2008).
- [9] Z. Chen, B. Nadal, B. Mahler, H. Aubin, B. Dubertret, *Adv. Funct. Mater.* **24**, 295, (2014).
- [10] B. Mahler, P. Spinicelli, S. Buil, X. Quelin, J. P. Hermier, B. Dubertret, *Nat. Mater.* **7**, 659, (2008).
- [11] J. Q. Grim, S. Christodoulou, F. Di Stasio, R. Krahne, R. Cingolani, L. Manna, I. Moreels, *Nat. Nanotech.* **9**, 891, (2014).
- [12] A. W. Achtstein, A. Schliwa, A. Prudnikau, M. Hardzei, M. V. Artemyev, C. Thomsen, U. Woggon, *Nano Lett.* **12**, 3151, (2012).
- [13] S. Ithurria, M. D. Tessier, B. Mahler, R.P.S.M. Lobo, B. Dubertret, Al. L. Efros, *Nature Mater.* **10**, 936, (2011).
- [14] B. Mahler, B. Nadal, C. Bouet, G. Patriarche, B. Dubertret, *J. Am. Chem. Soc.* **134**, 18591, (2012).
- [15] M. D. Tessier, P. Spinicelli, D. Dupont, G. Patriarche, S. Ithurria, B. Dubertret, *Nano Lett.* **14**, 207, (2014).
- [16] L. Biadala, F. Liu, M. D. Tessier, D. R. Yakovlev, B. Dubertret, M. Bayer, *Nano Lett.* **14**, 1134, (2014).
- [17] M. Pelton, S. Ithurria, R. D. Schaller, D. S. Dolzhenkov, D. V. Talapin, *Nano Lett.* **12**, 6158, (2012).
- [18] C. She, I. Fedin, D. S. Dolzhenkov, A. Demortiere, R. D. Schaller, M. Pelton, D. V. Talapin, D. Richard, *Nano Lett.* **14**, 2772, (2014).
- [19] B. Guzelturk, Y. Kalestimur, M. Olutas, S. Delikanli, H. V. Demir, *ACS Nano* **8**, 6599, (2014).
- [20] M. J. Bruchez, M. Moronne, P. Gin, S. Weiss, A. P. Alivisatos, *Science* **281**, 2013, (1998).
- [21] L. T. Kunneman, J. M. Schins, S. Pedetti, H. Heuclin, F. C. Gromeza, A. J. Houtepen, B. Dubertret, L.D.A. Siebbeles, *Nano Lett.* **14**, 7039, (2014).
- [22] B. Abecassis, M. D. Tessier, P. Davidson, B. Dubertret, *Nano Lett.* **14**, 710, (2013).
- [23] E. Baghani, S. K. O'Leary, I. Fedin, D. V. Talapin, M. Pelton, *J. Phys. Chem. Lett.* **6**, 1032, (2015).
- [24] M. D. Tessier, B. Mahler, B. Nadal, H. Heuclin, S. Pedetti, B. Dubertret, *Nano Lett.* **13**, 3321, (2013).
- [25] M. Olutas, B. Guzelturk, Y. Kalestemur, A. Yeltik, S. Delikanli, H. V. Demir, *ACS Nano* **9**, 5041, (2015).
- [26] R. Scott, A. W. Achtstein, A. Prudnikau, A. Antanovich, S. Christodoulou, I. Moreels, M. Artemyev, U. Woggon, *Nano Lett.* **15**, 4985 (2015).
- [27] A. S. Selyukova, A. A. Isaev, A. G. Vitukhnovsky, V. L. Litvak, A. V. Katsaba, V. M. Korshunov, R. B. Vasiliev, *Semicond.* **50**, 947 (1016).
- [28] J. Heckmann, R. Scott, A. V. Prudnikau, A. Antanovich, N. Owschimikow, M. Artemyev, J. I. Climente, U. Woggon, N. B. Grosse, A. W. Achtstein, *Nano Lett.* **17**, 6321 (2017).
- [29] S. Ithurria, D.V. Talapin *J. Am. Chem. Soc.* **134**, 18585, (2012).
- [30] R. Benchamekh, N. A. Gippius, J. Even, M. O. Nestoklon, J.-M. Jancu, S. Ithurria, B. Dubertret, Al. L. Efros, P. Voisin, *Phys. Rev. B* **89**, 035307, (2014).
- [31] A. M. Smirnov, A. D. Golinskaya, K. V. Ezhova, M. V. Kozlova, V. N. Mantsevich, V. S. Dneprovskii, *JETP* **125**, 890, (2017).
- [32] E. M. Garmire and A. Kost *Nonlinear optics in Semiconductors* (Academic, San Diego, 1999).
- [33] D. Lee, J. E. Zucker, A. M. Johnson, R. D. Feldman, R. F. Austin, *Appl. Phys. Lett.* **57**, 1132, (1990).
- [34] F. Tassone, Y. Yamamoto, *Phys. Rev. B* **59**, 10830, (1999).
- [35] A. Miller, P. Riblet, M. Mazilu, S. White, T. M. Holden, A. R. Cameron, P. Perozzo, *J. Appl. Phys.* **86**, 3734, (1999).
- [36] E. V. Shornikova, L. Biadala, D. R. Yakovlev, V. F. Sapega, Y. G. Kusrayev, A. A. Mitioglu, M. V. Ballottin, P. C. M. Christianen, V. V. Belykh, M. V. Kochiev, N. N. Sibeldin, A. A. Golovatenko, A. V. Rodina, N. A. Gippius, A. Kuntzmann, Ye Jiang, M. Nasilowski, B. Dubertret and M. Bayer, *Nanoscale* **10**, 646 (2018).
- [37] S. Schmitt-Rink, D. S. Chemla, D. A. B. Miller, *Phys. Rev. B* **32**, 6601, (1985).
- [38] E. L. Ivchenko *Optical spectroscopy of semiconductor nanostructures* (Alpha Science Int., Harrow, UK, 2005).
- [39] A. Kavokin, J. J. Baumberg, G. Malpuech, and F. P. Laussy, *Microcavities* (Oxford University Press, Oxford, 2007).
- [40] I. A. Yugova, M. M. Glazov, E. L. Ivchenko, Al. L. Efros, *Phys. Rev. B* **80**, 104436 (2009).
- [41] E. L. Ivchenko, V. P. Kochereshko, A. V. Platonov, D. R. Yakovlev, A. Waag, W. Ossau, and G. Landwehr, *Phys. Solid State* **39**, 1852 (1997).
- [42] M. D. Tessier, C. Javaux, I. Maksimovic, V. Loriette, B. Dubertret, *ACS Nano* **6**, 6751, (2012).
- [43] S. Shokhovets, O. Ambacher, B. K. Meyer, G. Gobsch, *Phys. Rev. B* **78**, 035207, (2008).